Research Square

Preprints are preliminary reports that have not undergone peer review.
They should not be considered conclusive, used to inform clinical practice,
or referenced by the media as validated information.

Comparative Transcriptome Analysis of Stem Hooks and Peduncles at Different Developmental Stages in Uncaria rhynchophylla

Jie Shen
Guangxi Medical University
Ya Qin
Guangxi Key Laboratory of High-Quality Formation and Utilization of Dao-di Herbs, Guangxi Botanical Garden of Medicinal Plants
Yuqiong Li
Guangxi Key Laboratory of High-Quality Formation and Utilization of Dao-di Herbs, Guangxi Botanical Garden of Medicinal Plants
Wenjing Liang
Guangxi Key Laboratory of High-Quality Formation and Utilization of Dao-di Herbs, Guangxi Botanical Garden of Medicinal Plants
Linxuan Li
Guangxi Key Laboratory of High-Quality Formation and Utilization of Dao-di Herbs, Guangxi Botanical Garden of Medicinal Plants
Cuihong Yang
Guangxi Key Laboratory of High-Quality Formation and Utilization of Dao-di Herbs, Guangxi Botanical Garden of Medicinal Plants
Qi Tang
College of Horticulture, National Research Center of EngineeringTechnology for Utilization of Botanical Functional Ingredients, Yuelushan Lab, Hunan Agricultural University
Lingjian Gui
Guangxi Key Laboratory of High-Quality Formation and Utilization of Dao-di Herbs, Guangxi Botanical Garden of Medicinal Plants
Haixia Yu
Guangxi Key Laboratory of High-Quality Formation and Utilization of Dao-di Herbs, Guangxi Botanical Garden of Medicinal Plants
Yuan Huang
Guangxi Key Laboratory of High-Quality Formation and Utilization of Dao-di Herbs, Guangxi Botanical Garden of Medicinal Plants
Guiyu Tan

Guangxi Key Laboratory of High-Quality Formation and Utilization of Dao-di Herbs, Guangxi Botanical Garden of Medicinal Plants

Shugen Wei

Guangxi Key Laboratory of High-Quality Formation and Utilization of Dao-di Herbs, Guangxi Botanical Garden of Medicinal Plants

Fang Qin

Guangxi Key Laboratory of High-Quality Formation and Utilization of Dao-di Herbs, Guangxi Botanical Garden of Medicinal Plants

Lingyun Wan

wanlingyun1984@163.com

Guangxi Key Laboratory of High-Quality Formation and Utilization of Dao-di Herbs, Guangxi Botanical Garden of Medicinal Plants

---

Research Article

Keywords: Uncaria rhynchophylla, stem hook, peduncle, organ differentiation, transcriptome, flowering regulation

Posted Date: November 25th, 2026

DOI: https://doi.org/10.21203/rs.3.rs-11534816/v1

License: This work is licensed under a Creative Commons Attribution 4.0 International License. Read Full License

Additional Declarations: No competing interests reported.

Comparative Transcriptome Analysis of Stem Hooks and Peduncles at Different Developmental Stages in *Uncaria rhynchophylla*

Jie Shen[1], Ya Qin[2,3,4], Yuqiong Li[2,3,4], Wenjing Liang[2,3,4], Linxuan Li[2,3,4], Cuihong Yang[2,3,4], Qi Tang[5], Lingjian Gui[2,3,4], Haixia Yu[2,3,4], Yuan Huang[2,3,4], Guiyu Tan[2,3,4], Shugen Wei,[1,2,3,4], Fang Qin*[2,3,4], Lingyun Wan*[1,2,3,4].

[1]Guangxi Medical University, Nanning 530021, China

[2]Guangxi Key Laboratory of High-Quality Formation and Utilization of Dao-di Herbs, Guangxi Botanical Garden of Medicinal Plants, Nanning 530023, China

[3]Guangxi Traditional Chinese Medicine Breeding Technology Innovation Center, Guangxi Botanical Garden of Medicinal Plants, Nanning 530023, China

[4]National Center for Traditional Chinese Medicine (TCM) Inheritance and Innovation, Guangxi Botanical Garden of Medicinal Plants, Nanning 530023, China

[5]College of Horticulture, National Research Center of EngineeringTechnology for Utilization of Botanical Functional Ingredients, Yuelushan Lab, Hunan Agricultural University, Changsha 410128, China

*Corresponding authors.

E-maile: qinfang200@163.com; wanlingyun1984@163.com

ORCID: 0000-0002-1780-0413(Lingyun Wan)

Abstract:*Uncaria rhynchophylla* is a widely used medicinal material in traditional Chinese medicine, and only its dried hook-bearing stem branches are legally recognized as the medicinal part. The stem hook and its homologous organ, the peduncle, differ markedly in morphology, physiological function, and secondary metabolite accumulation. However, the molecular regulatory mechanisms underlying their organ differentiation and developmental specialization remain unclear. Here, transcriptome sequencing was conducted during the stem-hook FAH and SAH stages, as well as the peduncles at FFH, SFH, and TFH stages. The results showed that hook maturation was characterized by cell wall biosynthesis and the phenylpropanoid pathway enrichment, accompanied by auxin signaling activation and abscisic acid (ABA) signaling attenuation. Whereas peduncle development was associated mainly with sugar metabolism and hormone signal transduction. Thus, the differentiation of the homologous stem hook and the peduncle was associated mainly with hormone signal transduction and transcription factor regulation with floral development orthologs. *UrFT, UrSOC1, UrFD, and UrAP1* were significantly upregulated in the flower-bud (FFH) and the floral repressor *UrSVP* was highly expressed in stem hooks. Weighted gene co-expression network analysis (WGCNA) identified a flower bud specific co-expression module with *UrAP1* as its hub gene, *UrAP1* localized to the nucleus, and Y1H assays showed that *UrFD* binds the *UrAP1* promoter, indicating that *UrAP1* is putatively transcriptionally regulated by *UrFD*. These findings provide insights into the mechanisms underlying the fate divergence of these homologous organs and provide a basis for the targeted regulation of the medicinal organ and molecular breeding of *U. rhynchophylla*.

Keywords: *Uncaria rhynchophylla*, stem hook, peduncle, organ differentiation, transcriptome, flowering regulation

1 Introduction

Uncaria rhynchophylla (Miq.) Miq. ex Havil. is a perennial woody vine belonging to the family Rubiaceae and one of the original plants of the traditional medicinal material “Gouteng” (National Pharmacopoeia Committee. 2025). Its dried hook-bearing stem branches are used medicinally, with the effects of extinguishing wind, arresting convulsions, clearing heat, and pacifying the liver (National Pharmacopoeia Committee. 2025). Modern pharmacological studies have demonstrated that the active constituents of *U. rhynchophylla* are mainly indole alkaloids, including rhynchophylline and isorhynchophylline (Liang et al. 2020; Guo et al. 2019). Through multiple mechanisms, including antagonism of calcium channels and modulation of neurotransmitter release, these bioactive compounds exhibit pronounced antihypertensive, anticonvulsant, neuroprotective, and sedative-hypnotic effects (Yang et al. 2020; Qin et al. 2024), and they have clear clinical value in treating primary hypertension, vascular dementia, Parkinson's disease, and other neurological disorders (Kuang et al.

2024; Cao et al. 2024). Moreover, the alkaloids of *U. rhynchophylla* show pronounced tissue-specific distribution with alkaloid content and composition differing markly among organs, accordingly, only the dried hook-bearing stem branches are officially recognized as the medicinal part of “Gouteng” in the Chinese Pharmacopoeia, whereas the peduncle is not used medicinally (Cao et al. 2024).

From a developmental-biology perspective, both the stem hook and the peduncle of *U. rhynchophylla* originate from axillary meristems, yet their developmental fates diverge completely (Wan et al. 2025). The stem hook is a specialized climbing vegetative organ, after perceiving mechanical stimuli, the axillary meristem undergoes asymmetric growth to form a hook-like structure, and its development is accompanied by vigorous secondary wall deposition and lignification together with highly developed vascular tissues (Deng et al. 2021) The NAC and MYB transcription-factor families are core regulators of secondary-cell-wall synthesis; they activate key lignin-biosynthetic genes such as *CAD* and *CCoAOMT* and mediate xylem differentiation and secondary-wall thickening (Zhong et al. 2021; Zhang et al. 2025). As a reproductive support organ, the peduncle provides mechanical support and conducts water, mineral elements and assimilates in addition to supplying nutrients to floral organs, it exhibits a low degree of lignification, and its development is tightly coupled to the flowering program. The photoperiod pathway is one of the key signaling cascades controlling flowering time, in which *GIGANTEA (GI)*, *CONSTANS (CO)*, and the florigen *FLOWERING LOCUS T (FT)* constitute the core regulatory hierarchy (Abe et al. 2005), whereas the MADS-box transcription-factor family determines floral organ identity and regulates the differentiation of sepals, petals, stamens, and carpels (Wu et al. 2025). However, whether these core flowering genes participate in regulating the development and differentiation of the peduncle remains unknown. Although both the stem hook and the peduncle are derived structures of the stem, their pronounced differences in morphogenesis, physiological function, and secondary metabolite accumulation make them ideal materials for studying the fate divergence of plant homologous organs.

In recent years, RNA sequencing (RNA-Seq) has emerged as a powerful tool for revealing genome wide gene expression dynamics and has been successfully applied to studies of organ differentiation in numerous medicinal plants. For example, comparative transcriptome analyses have clarified the divergent developmental fates of the homologous tendril and inflorescence primordia in *Vitis vinifera* (Díaz-Riquelme et al. 2014), dissected the mechanisms underlying the divergent seed-dispersal fates of aerial and subterranean fruits in *Cardamine chenopodiifolia* (Emonet et al. 2024), and identified key regulators of thorn tip sclerification in *Citrus* (Ren et al. 2025).Accordingly, the present study took *U. rhynchophylla* stem hooks (young stage, FAH; mature stage, SAH) and peduncles (flower-bud stage, FFH; semi-flowering stage, SFH; full-flowering stage, TFH) as experimental materials, and performed transcriptome sequencing on the Illumina high-throughput platform (Reuter et al. 2015). Stem hooks were sampled at two stages representing vegetative development of the climbing organ, whereas peduncles were sampled at three stages spanning the flower-bud to full-flowering transition to capture the reproductive program, this design allowed both within organ developmental comparisons and cross organ comparisons of the two homologous structures. By integrating differential gene screening, GO/KEGG enrichment analysis, STEM time-course clustering, and weighted gene co-expression network analysis (WGCNA), we characterized transcriptome reprogramming in these two homologous organs. Candidate genes related to flower development were selected and functionally validated by real-time quantitative PCR (qRT-PCR), subcellular localization, and a yeast one-hybrid (Y1H) assay. This study aimed to identify key differentially expressed genes and core regulatory modules between stem hooks and peduncles, to elucidate the molecular regulatory differences between *U. rhynchophylla* stem hooks and their homologous peduncles during development, and to provide a theoretical basis for elucidating the fate divergence mechanisms of homologous structures and for targeted regulation of the medicinal organ.

2 Materials and Methods

2.1 Plant materials and sample preparation

Plant materials were collected from the *Uncaria* (gambir plant) cultivation base in Sanchadun, Mabucun, Banlan Town, Rong'an County, Liuzhou City, Guangxi, China (25°28′ N, 109°37′ E). Healthy, disease and pest-free adult *U. rhynchophylla* plants were selected. Stem hooks at the young stage (FAH) and mature stage (SAH) were sampled from vegetative branches as hook samples at different developmental stages (AH) (Fig. 1A). Peduncles at the flower-bud stage (FFH), semi-flowering stage (SFH), and full-flowering stage (TFH) were sampled from reproductive branches as peduncle samples at different developmental stages (FH) (Fig. 1B). All floral buds, flowers, and inflorescence axes were carefully removed from each peduncle sample, only the peduncle stalk was retained. Three biological replicates were collected for each stage. Immediately after collection, samples were flash-frozen in liquid nitrogen and then stored at -80 °C until RNA extraction.

Sampling was permitted by the management of the cultivation base, and all sampling procedures complied with relevant national legislation of China.

The plant materials of *Uncaria rhynchophylla* used in this study were collected from the cultivated nursery base in Sanchadun, Mabucun, Banlan Town, Rong'an County, Liuzhou City, Guangxi, China. Sampling was permitted by the management of the nursery base. All sampling procedures complied with relevant national legislation of China. No wild protected plant resources were involved in this study.

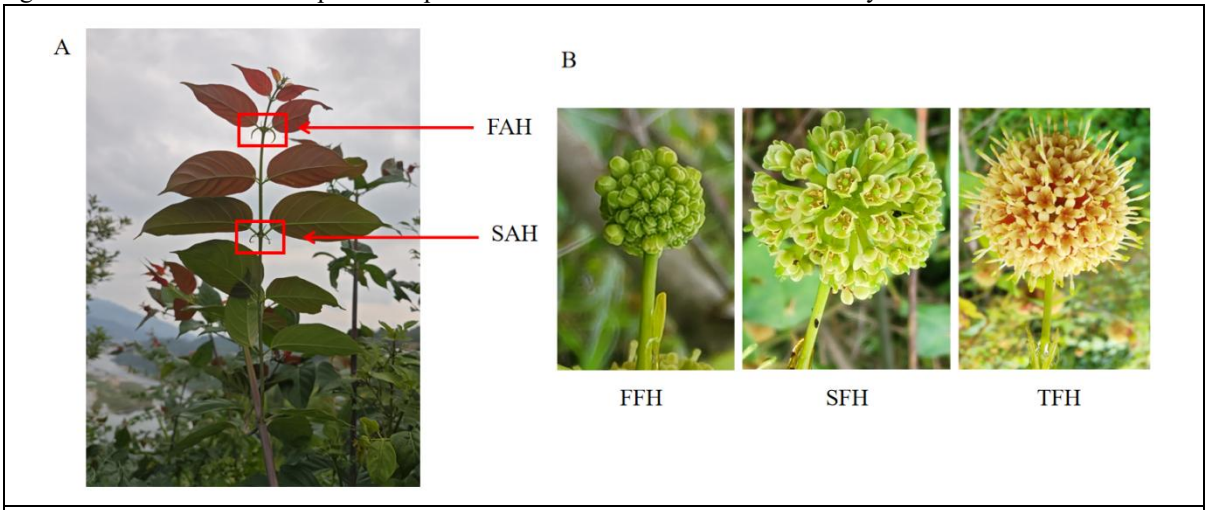


Fig 1: Morphological characteristics of *Uncaria rhynchophylla* stem hooks and peduncles at different developmental stages. A: Stem hooks at the young stage (FAH) and mature stage (SAH). B: Peduncles at the flower-bud stage (FFH), semi-flowering stage (SFH), and full-flowering stage (TFH).

2.2 Total RNA extraction and construction of transcriptome-sequencing libraries

Total RNA was extracted from 50-100 mg of liquid-nitrogen-ground samples using the RNAprep Pure Plant Kit (TIANGEN, Beijing, China) according to the manufacturer's instructions. RNA purity was assessed using a Kaiao K5500® Spectrophotometer (Kaiao, Beijing, China), with A260/A280 ratios between 1.8 and 2.2 and A260/A230 ratios above 2.0, and RNA integrity was verified using an Agilent 2100 Bioanalyzer (Agilent Technologies, CA, USA); all samples exhibited an RNA Integrity Number (RIN) ≥ 8.0. Qualified RNA samples were used to construct strand-specific cDNA libraries using the NEBNext® Ultra™ II Directional RNA Library Prep Kit for Illumina® (New England Biolabs, MA, USA) according to the manufacturer's instructions. Fifteen libraries were sequenced on an Illumina HiSeq 2500 platform by Wuhan Benagen Tech Solutions Company Limited.

2.3 Bioinformatic analysis

2.3.1 Quality control and reference-genome alignment

To ensure the reliability of downstream analyses, raw sequencing data were first subjected to stringent quality control. Raw reads were filtered using FASTQ (Cock et al. 2010) to remove adaptor sequences, low-quality reads, reads with an N content > 5%, and polyA-contaminated reads, yielding high-quality clean reads. Clean reads were aligned to the *U. rhynchophylla* reference genome (Mu et al. 2026) using STAR (v.2.7.0.d) (Dobin et al. 2013); alignment statistics and sequencing-quality evaluation were performed using Qorts (1.3.0) (Hartley et al. 2015).

2.3.2 Transcript assembly and quantification of gene expression

Reference genome-based transcript assembly was performed using StringTie v 1.0 (Pertea et al. 2015), and a GTF transcript annotation file was output. Read counts for each gene in every sample were calculated using featureCounts and used for subsequent expression quantification.

2.3.3 Identification of differentially expressed genes

Differentially expressed genes (DEGs) were identified using DESeq2 (Anders et al. 2010), with a threshold of q-value < 0.05 and $|\log_2 \text{FoldChange}| > 1$.

2.3.4 Gene Ontology and KEGG pathway enrichment analyses

Gene Ontology (GO) and KEGG pathway enrichment analyses were performed using clusterProfiler (Ashburner et al. 2000; Kanehisa et al. 2008; Xu et al. 2024); adjusted p-value < 0.05 was considered to indicate significant enrichment. GO terms were divided into three categories: molecular function, cellular component, and biological process. KEGG analysis was used to resolve the metabolic and signaling pathways in which DEGs were involved.

2.3.5 Identification and analysis of flowering-related genes

Flowering-related genes were identified on two fronts. First, based on NR, Swiss-Prot, eggNOG, and InterProScan annotations, flowering-related genes were retrieved using keywords such as “flower development”, “floral meristem”, and “flowering”. Second, using the protein sequences of *Arabidopsis thaliana* flowering-pathway genes as a database, BLASTp alignment (E-value ≤ 1×10^{-5}) was performed to identify orthologs of *AP1, SOC1, FLC, LFY, and FT*. Expression heatmaps were drawn based on the FPKM matrix.

2.4 qRT-PCR validation of transcriptome results

Sixteen differentially expressed genes (DEGs) were randomly selected for qRT-PCR validation, and gene-specific primers were designed using Primer Premier 5.0 software (Singh et al. 1998). Total RNA was reverse-transcribed into cDNA using the HiScript® Ⅲ 1st Strand cDNA Synthesis Kit (+gDNA wiper) (Vazyme, Nanjing, China) according to the manufacturer's instructions. qRT-PCR amplification was performed on a QuantStudio™ X Real-Time PCR System (Thermo Fisher Scientific, MA, USA) using the ChamQ Universal SYBR qPCR Master Mix (Vazyme, Nanjing, China). S-adenosylmethionine decarboxylase (SAM) (Liu et al. 2025; Shao et al. 2024) was used as the internal reference gene, and relative gene expression levels were calculated using the $2^{-\Delta\Delta Ct}$ method (Dai et al. 2019). Three biological replicates were analyzed for each sample. The primer sequences are listed in Online Resource 1.

2.5 STEM time-course expression analysis

To characterize the temporal expression dynamics of genes during peduncle development, Short Time-series Expression Miner (STEM) software (Zhao et al. 2024; Ernst et al. 2006) was used to perform time-course expression clustering. Genes with an FPKM > 1 in at least one of the three developmental stages were retained, and their expression values were log2-transformed and normalized prior to clustering. Using STEM, each gene was assigned to the predefined model profile that best matched its expression trajectory, and the significance of each profile was evaluated by the permutation-based test implemented in STEM; profiles with a corrected P-value < 0.05 were considered significantly enriched and retained for further analysis. Genes assigned to the same significant profile were regarded as sharing a common temporal expression pattern during peduncle development, and model profiles showing continuous up or down regulation were further mined to screen candidate transcription factors and hub genes associated with peduncle development.

2.6 Weighted gene co-expression network analysis (WGCNA)

Genes with FPKM > 1 and detectable expression in at least one sample were used to construct the co-expression network. The soft-thresholding power β was set to 18, and an adjacency matrix and a topological overlap matrix (TOM) were constructed. The parameters minModuleSize = 30 and deepSplit = 2 were used, and co-expression modules were identified by dynamic tree cutting. Module eigengenes were calculated, and key transcription factors involved in flower development were mined by integrating module-trait associations and hub-gene annotation.

2.7 Cloning and functional validation of candidate genes *UrAP1* and *UrFD*

2.7.1 Subcellular localization

The full-length CDS of *UrAP1* was obtained and used to construct an *UrAP1*-GFP fusion expression vector. The construct was introduced into *Agrobacterium tumefaciens*, which was then used for transient infiltration of *Nicotiana benthamiana* leaves. Green fluorescent protein (GFP) signals were observed by laser confocal scanning microscopy 48-72 h after infiltration.

2.7.2 Cloning of the *UrAP1* promoter and construction of the bait vector

Genomic DNA was extracted from *U. rhynchophylla*, and an approximately 2000 bp promoter sequence upstream of the *UrAP1* ATG start codon was amplified. The amplicon was recovered from an agarose gel, purified, and verified by sequencing. The pAbAi vector was digested with BstbI, and the purified promoter fragment was inserted by one-step cloning to generate the bait vector pAbAi-*UrAP1*. Specific primers for the *UrAP1* promoter are listed in Online Resource 2.

2.7.3 Cloning of *UrFD* and construction of the prey plasmid

Total RNA was extracted from *U. rhynchophylla* and reverse-transcribed into cDNA, from which the full-length CDS of *UrFD* was amplified. The pGADT7 vector was digested with BamHI, and the *UrFD* CDS was inserted by one-step cloning to generate the prey plasmid pGADT7-*UrFD*, which was confirmed by sequencing. Specific primers for the full-length *UrFD* sequence are listed in Online Resource 3.

2.7.4 Yeast one-hybrid assay

An Y1HGold-pAbAi yeast one-hybrid system was used to verify the interaction between *UrFD* and the *UrAP1* promoter. The bait plasmid was linearized and transformed into Y1HGold competent cells, and positive bait strains were selected on SD/-Ura medium. The Aureobasidin A (AbA) concentration required to suppress

self-activation was determined. The prey plasmid pGADT7-*UrFD* was then transformed into bait competent cells, with p53-AbAi + pGADT7-p53 as the positive control and p53-AbAi + empty pGADT7 as the negative control. Yeast cultures were adjusted to an OD600 gradient, serially diluted, and spotted onto SD/-Leu plates and SD/-Leu plates containing the optimal AbA concentration. Plates were incubated at 30 °C for 2-5 d, and yeast growth was observed.

3 Results

3.1 Quality of transcriptome data and overall characteristics of the samples

Transcriptome sequencing was performed on five stages of *U. rhynchophylla*, namely stem hooks (FAH, SAH) and peduncles (FFH, SFH, TFH), with three biological replicates per stage. For each sample, 38.77-51.83 million clean reads were obtained; the Q30 base percentage exceeded 93.61%, and the unique genome-mapping rate exceeded 89.51%, indicating that the sequencing data were of reliable quality (Online Resource 4).

Sample-correlation analysis showed high correlation coefficients among biological replicates within each group, indicating good repeatability(Fig. 2A). The correlation between FFH and SFH was relatively low, whereas that between SFH and TFH was high, indicating that a dramatic transcriptional change occurred during the transition from the flower-bud stage to the semi-flowering stage, whereas the transcriptional change from semi-flowering to full flowering was modest. Principal component analysis (PCA) showed that PC1 explained 26.55% of the variance and PC2 explained 21.12%(Fig. 2B). Stem-hook samples clustered together, whereas peduncle samples were arranged in the order FFH-SFH-TFH. Both organ identity and developmental timing jointly drove sample separation, supporting the reliability of sample grouping.

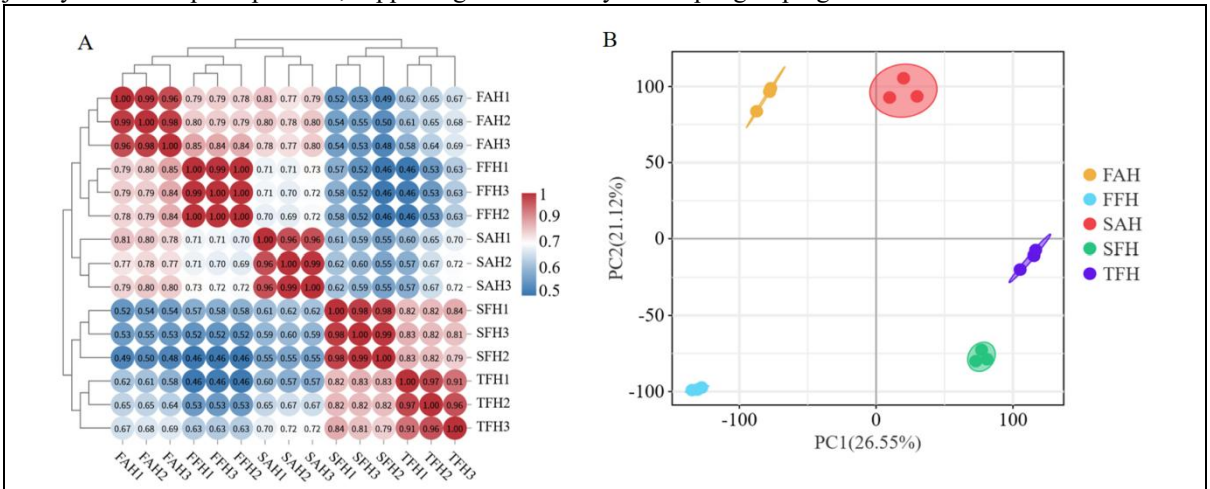


Fig. 2: Sample correlation analysis of *Uncaria rhynchophylla* stem hooks and peduncles at different developmental stages. A: Correlation analysis of the sequenced samples. The dendrogram on the left and top shows sample clustering; sample names are displayed on the right and bottom; colored blocks indicate the magnitude of correlation between each pair of samples, with different colors representing high and low correlation. B: Principal component analysis (PCA) of the sequenced samples. The horizontal axis represents the first principal component (PC1) and the vertical axis represents the second principal component (PC2). Different shapes denote different samples, and different colors denote different groups.

3.2 Identification of DEGs reveals transcriptional differences underlying organ differentiation and developmental transitions

Using q-value < 0.05 and $|\log_2\text{FoldChange}| > 1$ as thresholds, five key comparison groups were set up: the hook-development transition FAH vs SAH, the organ-fate divergence FAH vs FFH, and three peduncle time-course comparisons, FFH vs SFH, FFH vs TFH, and SFH vs TFH. DEGs in each group were obtained (Fig. 3A). There were 7058 DEGs in FAH vs SAH (2769 upregulated and 4289 downregulated), 8252 DEGs in FAH vs FFH (4866 upregulated and 3366 downregulated), 8999 DEGs in FFH vs SFH, 10894 DEGs in FFH vs TFH, and 6027 DEGs in SFH vs TFH. Except for FAH vs FFH, the number of downregulated genes in each comparison was markedly higher than that of upregulated genes. A Venn diagram (Fig. 3B) revealed 367 DEGs shared by all five comparisons, representing a conserved regulatory module shared during organ development. In this study, FAH vs SAH and FAH vs FFH were selected for GO and KEGG enrichment analyses, whereas peduncle developmental dynamics were resolved by STEM time-course clustering.

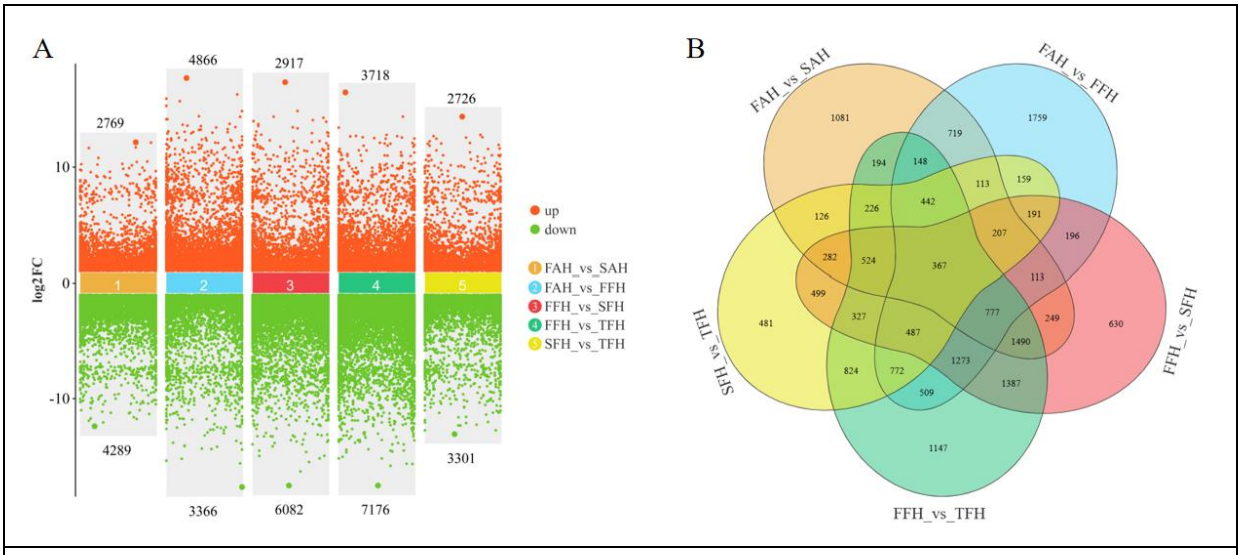
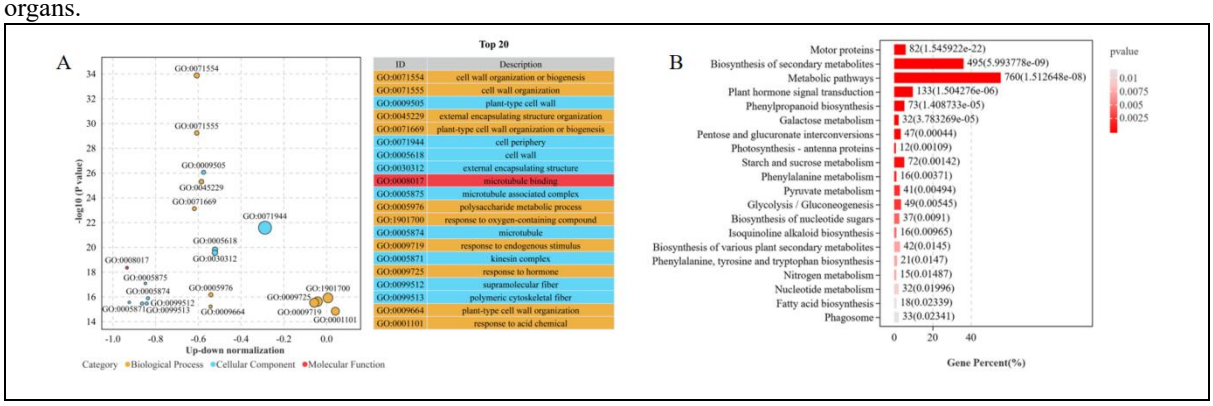


Fig. 3: Statistics of differentially expressed genes (DEGs) among *Uncaria rhynchophylla* stem hooks and peduncles at different developmental stages. A: Volcano/scatter plots of DEGs. B: Venn diagram showing DEGs shared across the five comparison groups.

3.3 GO and KEGG enrichment dissect pathway features of hook maturation and hook-peduncle differentiation

GO enrichment analysis of DEGs from FAH vs SAH (young to mature hooks) (Fig. 4A) showed significant enrichment in terms related to cell-wall organization and biogenesis, plant-type cell wall, microtubule binding, and kinesin complex, i.e, terms associated with cell-wall construction and cytoskeleton assembly. KEGG enrichment (Fig. 4B) showed significant enrichment of pathways related to motor proteins, biosynthesis of secondary metabolites, plant hormone signal transduction, phenylpropanoid biosynthesis, and starch and sucrose metabolism, indicating that hook maturation was accompanied by cell-wall construction, secondary-metabolite synthesis, and hormone-signal reprogramming.

GO enrichment of FAH vs FFH (young hooks vs flower-bud peduncles) (Fig. 4C) focused on terms such as hormone response, hormone-mediated signaling pathways, organ development, and transcription-factor activity; KEGG enrichment (Fig. 4D) highlighted plant hormone signal transduction, secondary-metabolite biosynthesis, the MAPK signaling pathway, and phenylpropanoid biosynthesis. These results indicate that hormone signal transduction and transcription-factor networks may be central to fate divergence between these two homologous organs.



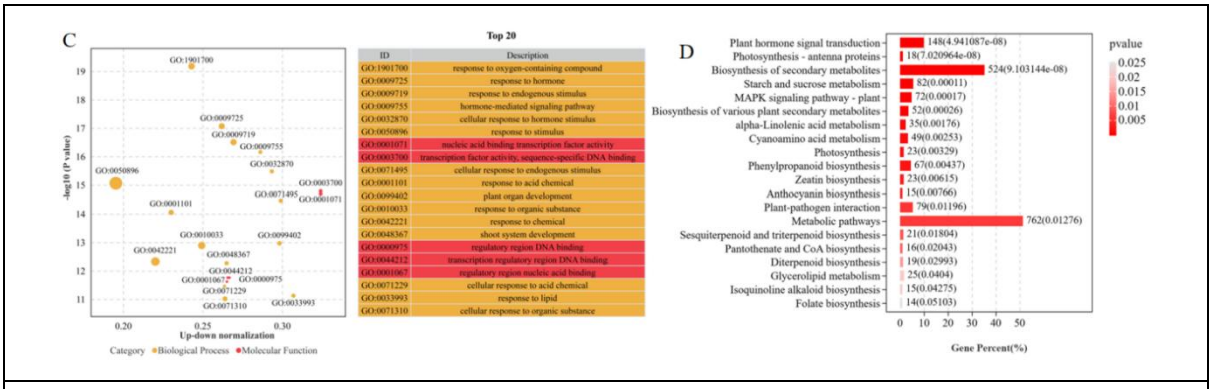


Fig. 4: GO and KEGG enrichment analyses of differentially expressed genes (DEGs) in *Uncaria rhynchophylla* stem hooks at different developmental stages. A、B: GO and KEGG enrichment results for the FAH vs SAH comparison. C、D: GO and KEGG enrichment results for the FAH vs FFH comparison.

3.4 Time-course clustering of peduncle genes resolves developmental dynamics of the reproductive support structure

Time-course trend clustering of DEGs across the peduncle developmental sequence (FFH-SFH-TFH) yielded eight expression profiles, four of which were statistically significant ($p < 0.05$): Profile 0 (2675 DEGs), Profile 1 (3059), Profile 6 (1934), and Profile 7 (1475) (Fig. 5). GO and KEGG enrichment analyses were performed for each significant profile.

Profiles 0 and 1 represent early transcriptional activity, with genes highly expressed at the flower-bud stage (FFH). Profile 0 genes were continuously downregulated from FFH to TFH and were enriched in cytoskeleton-related GO terms (microtubule, kinesin complex, cytoskeletal part) and KEGG pathways such as DNA replication, motor proteins, and starch and sucrose metabolism, indicating active cell division and tissue construction in the flower-bud peduncle (Online Resource 5). Profile 1 genes dropped sharply during the FFH→SFH transition and remained low; their GO terms centered on the cell wall and plasma membrane (cell periphery, plant-type cell wall, plasmodesma), with KEGG enrichment in phenylpropanoid, cutin/suberine/wax, and fatty acid elongation metabolism and ABC transporters (Online Resource 5).

By contrast, Profiles 6 and 7 were activated mainly during the SFH→TFH transition. Profile 6 genes increased markedly at SFH and were enriched in carbohydrate and heme-binding, glycosyltransferase, oxidoreductase, and UDP-glycosyltransferase activities, consistent with KEGG enrichment in secondary-metabolite pathways (isoquinoline alkaloid, phenylpropanoid, anthocyanin) and hormone modification, reflecting extensive activation of secondary-metabolite biosynthesis in late peduncle development (Online Resource 5). Profile 7, showing a similar upward trend, was enriched in unfolded-protein/chaperone binding and in KEGG pathways including protein processing in the endoplasmic reticulum and α-linolenic acid metabolism (Online Resource 5).

Starch and sucrose metabolism DEGs were concentrated in Profile 0 (32 genes), and plant-hormone signal-transduction DEGs were distributed across Profiles 0 (44) and 1 (51); both were downregulated during the FFH→SFH transition. These results indicate that temporal switching of sugar metabolism and hormone signal transduction is closely associated with the developmental transition of the peduncle during flowering.

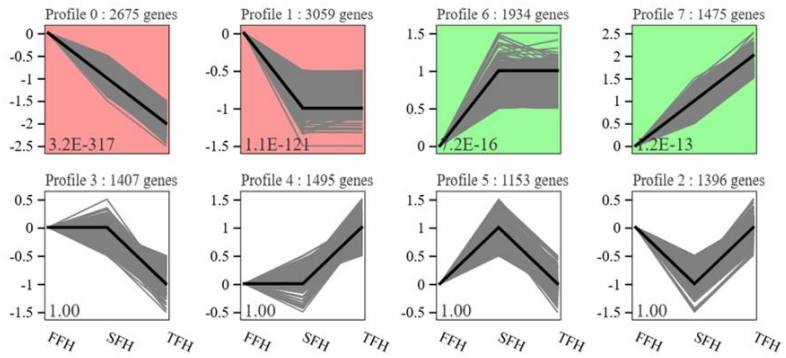


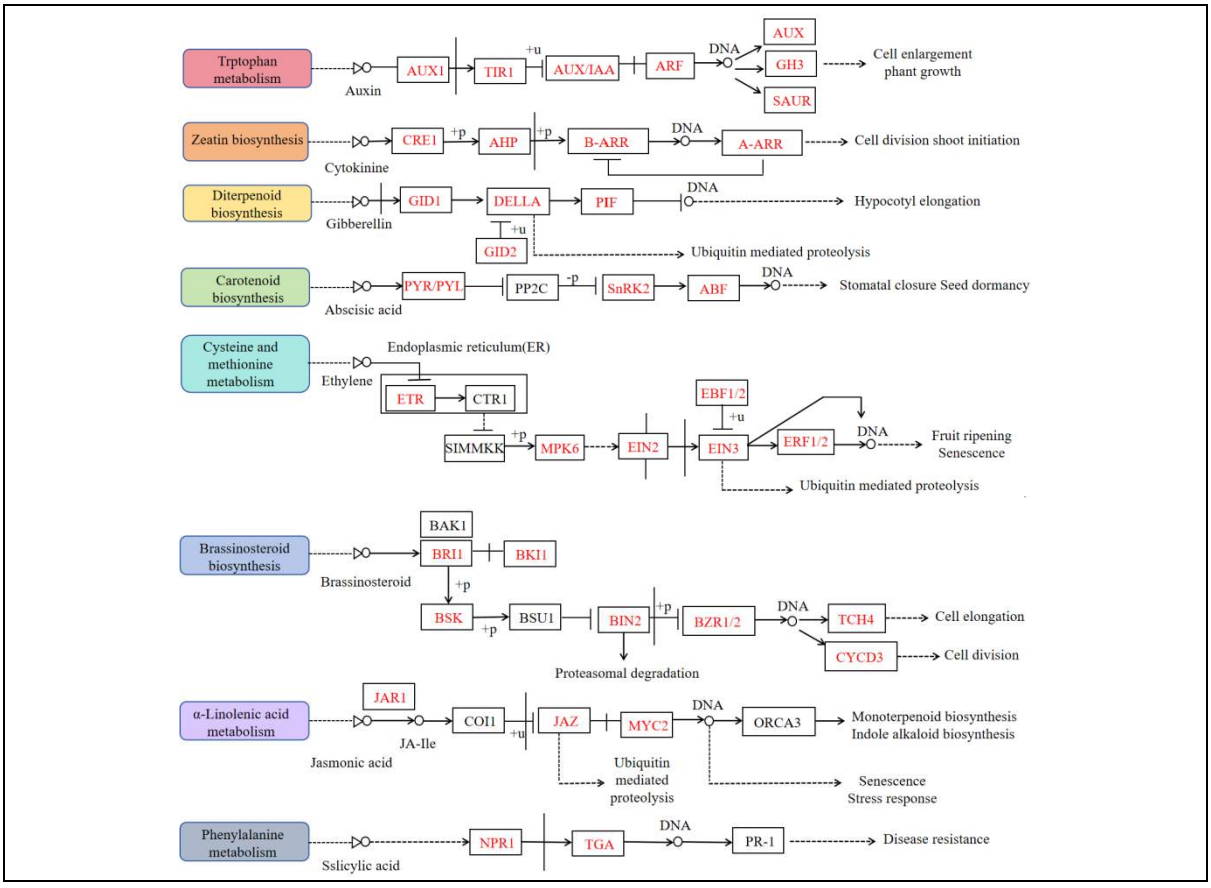
Fig. 5: STEM time-course expression profiles (trend clustering) of differentially expressed genes in *Uncaria rhynchophylla* peduncles.

3.5 Differential expression of genes in the plant hormone signal transduction pathway

To dissect how hormones mediate the divergent fates of the homologous stem hook and peduncle, DEGs in the KEGG plant hormone signal transduction pathway (ko04075) were analyzed. In total, 228 DEGs involved in auxin, GA, CK, ABA, ET, JA, SA, and BR signaling were identified, and their expression across the five stages (FAH, SAH, FFH, SFH, TFH) was visualized as a heatmap (Fig. 6).

Cross organ comparison revealed organ specific hormone signaling between the stem hook and peduncle. In the early organ identity comparison (FAH vs FFH), 123 hormone-signal-related DEGs were identified, and the two homologous organs showed strikingly different hormone response features. The GA pathway genes *GID2* and *DELLA* were expressed at significantly higher levels in the peduncle (FFH), indicating that activation of GA signaling is closely associated with the initiation of reproductive peduncle identity. By contrast, the cytokinin pathway *ARR-B* and ethylene pathway *EIN3* genes were preferentially expressed in the hook (FAH), reflecting that early hook development requires maintenance of relatively high CK and ethylene signaling to sustain the vegetative growth of the climbing organ. This divergence in GA versus CK/ethylene signaling may therefore represent a molecular signature distinguishing the reproductive peduncle from its homologous vegetative hook.

Temporal development is accompanied by stage specific hormone signaling reprogramming within each organ. During hook development from FAH to SAH, 113 hormone-signal-related DEGs were identified. The heatmap showed that most auxin pathway *SAUR* and *ARF* genes were highly abundant at SAH, whereas ABA pathway *ABF* genes maintained higher transcript levels at FAH and were downregulated upon entering SAH, indicating that activation of auxin signaling and attenuation of ABA signaling are important molecular features of hook morphogenesis. During peduncle time course development (FFH→SFH→TFH), 115 hormone-signal-related DEGs were assigned to Profiles 0, 1, 6, and 7 by STEM clustering. Genes such as *IAA* and *SAUR* in Profile 1 peaked at FFH and decreased progressively with peduncle development, suggesting that they are mainly involved in peduncle initiation and differentiation, whereas genes in Profile 6, such as *ABF, MYC2*, and *ERF1*, were continuously upregulated during SFH-TFH and may regulate peduncle elongation and late maturation.



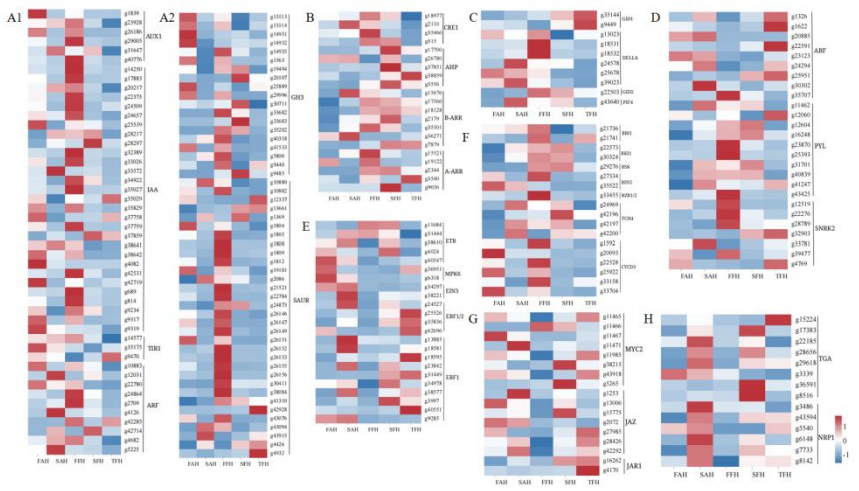
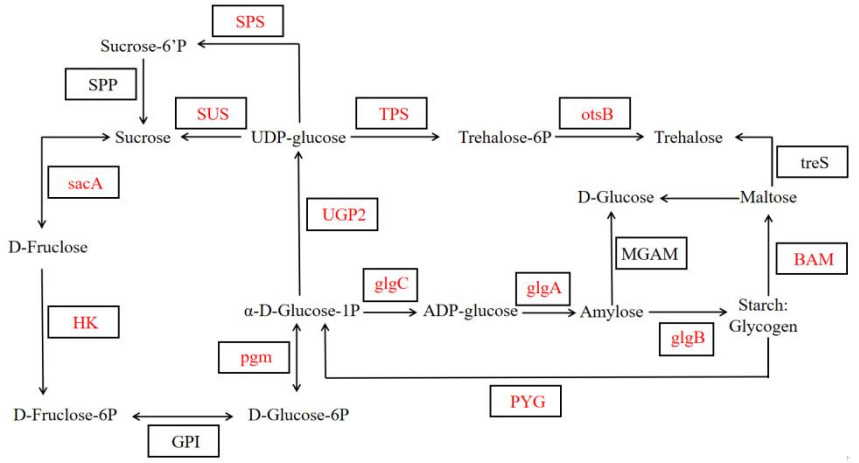


Fig. 6: Analysis of differentially expressed genes (DEGs) associated with the plant hormone signal transduction pathway and heatmap comparing the expression levels of hormone related genes. A1、A2: IAA;B: CTK; C: GA3; D: ABA; E: ETH; F: BR; G: JA; H: SA.

3.6 DEGs related to starch and sucrose metabolism

A total of 238 DEGs involved in starch and sucrose metabolism (ko00500) were identified across the five stages and visualized as a heatmap (Fig. 7). During hook development (FAH→SAH), sucrose-synthase *SUS* and β-glucosidase *BAM* genes were upregulated whereas hexokinase *HK* genes were downregulated, whereas in the hook and peduncle comparison (FAH vs FFH), *TPS* and the starch synthesis gene *glgC* were significantly upregulated in the flower-bud peduncle but *HK* and *SPS* genes were preferentially expressed in the hook. During peduncle development, genes for sucrose hydrolysis and glycosyltransferases were progressively upregulated toward flowering. These results indicate that the vegetative hook preferentially uses hexose metabolism to support rapid growth and lignification, whereas the reproductive peduncle first activates starch and trehalose synthesis and later mobilizes sucrose hydrolysis and glycosyltransfer to support flower-bud differentiation and floral organ maturation.



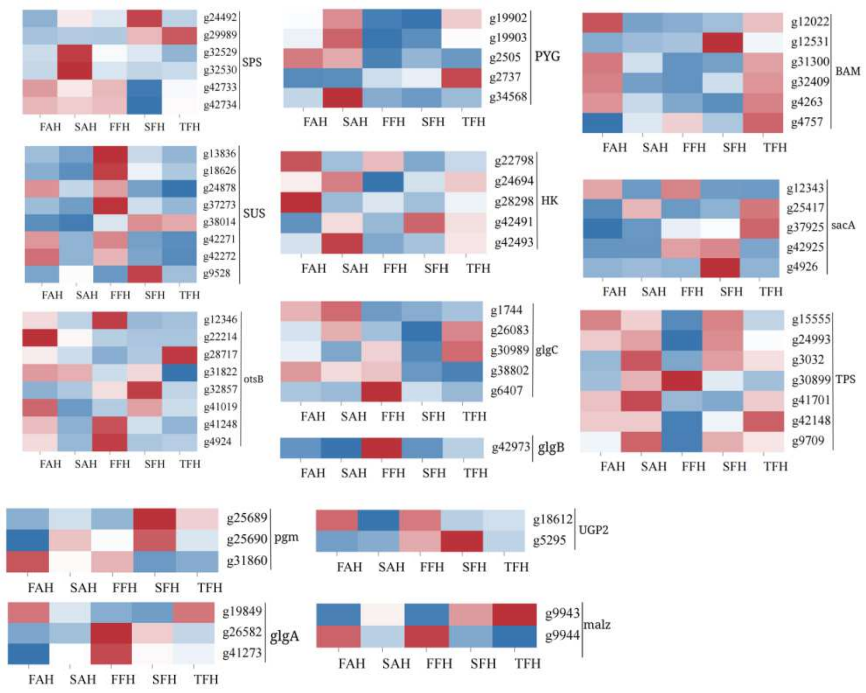


Fig. 7: Analysis of differentially expressed genes (DEGs) associated with starch and sucrose metabolism and a heatmap showing the expression levels of the corresponding genes.

3.7 Identification of flowering-related DEGs during floral induction

Transcriptional regulation is central to floral induction and the reproductive transition in *U. rhynchophylla*. GO enrichment indicated that a substantial number of differentially expressed genes were associated with transcription factor activity, and genes of several transcription factor families, including MADS-box, AP2/ERF, NAC, MYB, and bHLH, showed clear differential expression between stem hooks and peduncles, with some family members significantly upregulated during the reproductive transition, suggesting that transcription factor networks orchestrate the fate switch between these two homologous organs.

A total of 100 *U. rhynchophylla* orthologs related to flower development were identified, of which 46 were significantly differentially expressed (q-value < 0.05, |log2FC| > 1) during hook or peduncle development (Fig. 8). The heatmap jointly comparing all five stages showed that the florigen ortholog *UrFT*, the flowering integrators *UrSOC1* and *UrFD*, and the floral meristem identity gene *UrAP1* were highly expressed in the peduncle, especially at the flower-bud stage (FFH), indicating that these flowering promoting genes are strongly activated when the peduncle acquires a reproductive fate. By contrast, the floral repressor *UrSVP* was highly expressed in stem hooks, which may repress the expression of the flowering integrators *FT*, *SOC1*, and *LFY*, thereby restraining the floral program and maintaining the vegetative identity of the hook. Notably, several members within these MADS-box and bHLH families exhibited stage and tissue specific expression, further supporting their roles in the divergent development of the two organs.

This reciprocal expression of floral activators and repressors thus suggests an important role of flowering related genes in the fate transition between the vegetative hook and the reproductive peduncle.

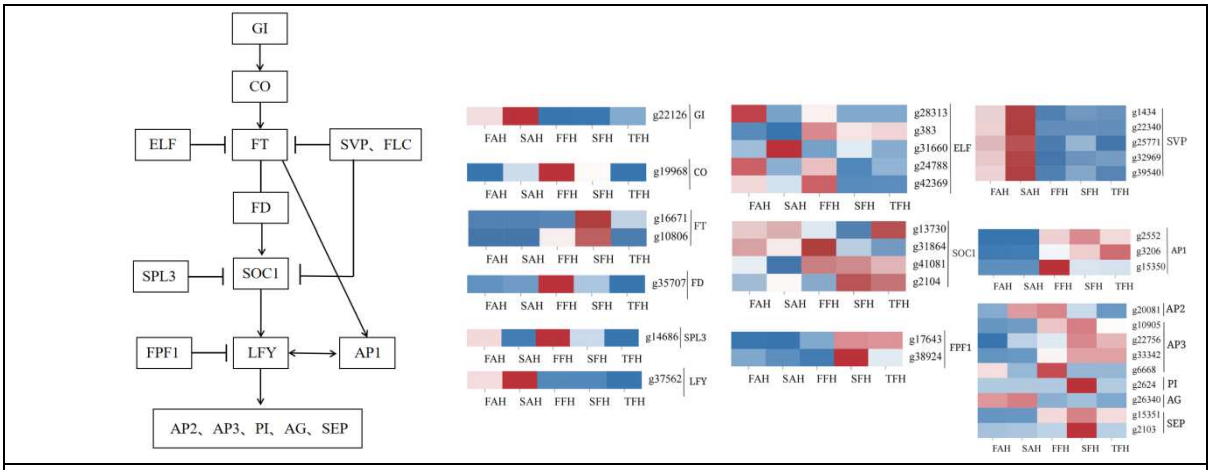
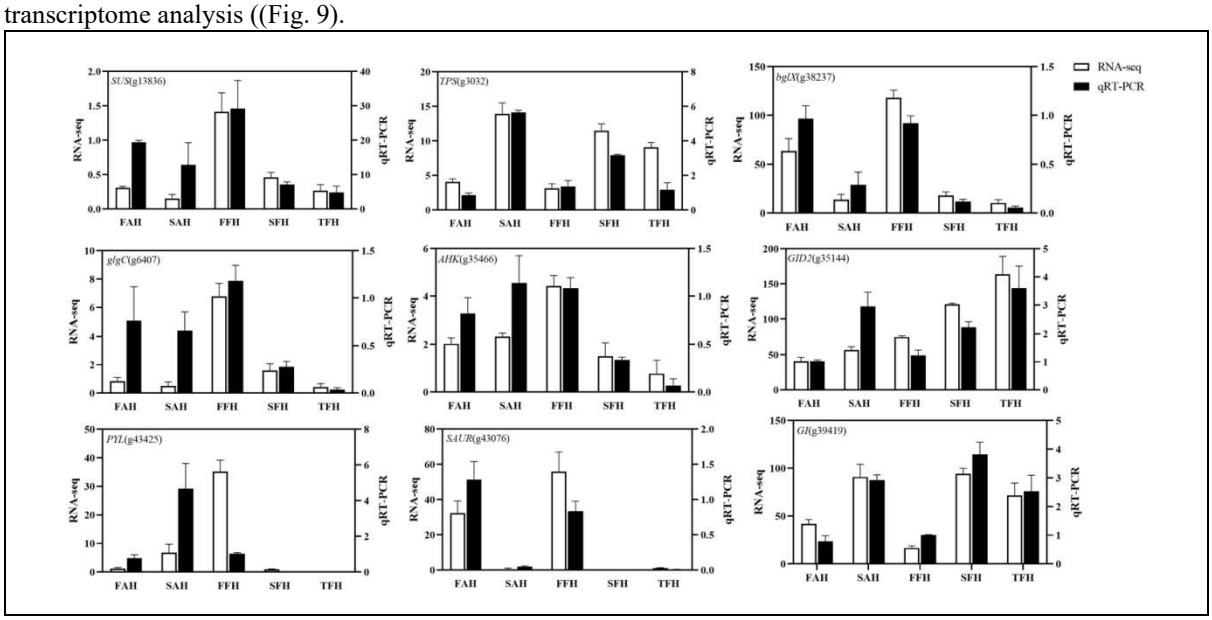


Fig. 8: Analysis of flowering-related differentially expressed genes (DEGs) during floral induction and a heatmap showing the expression levels of the corresponding genes.

3.8 qRT-PCR validation of RNA-Seq results

To further validate the RNA-Seq results, 16 DEGs across the five developmental stages were randomly selected and subjected to qRT-PCR based expression analysis in both *U. rhynchophylla* stem hooks and peduncles. The qRT-PCR results were highly consistent with the RNA-Seq data, confirming the accuracy of the transcriptome analysis ((Fig. 9).



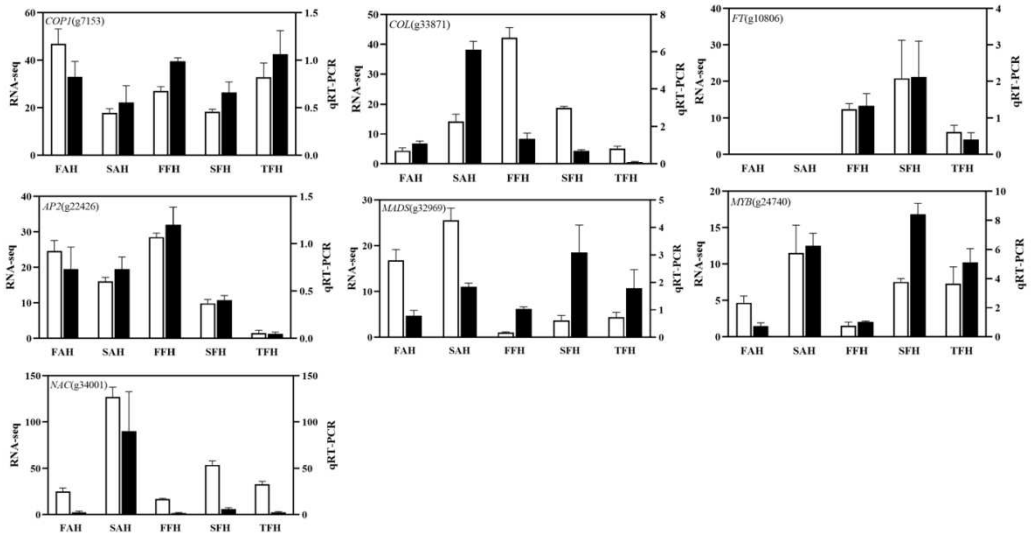


Fig. 9 Results of qRT-PCR verification of sequencing data. The X-axis represents 5 developmental stages, and the Y-axis represents the gene expression level. The white bars represent the sequencing data, and the black bars represent the quantitative data. The data were analyzed in 3 biological replicates, and the standard deviation is indicated by the error bars.

3.9 Weighted gene co-expression network analysis (WGCNA)

WGCNA with soft threshold β = 18 yielded 21 co-expression modules (27-2770 genes each) (Fig. 10). Each developmental stage was associated with a dedicated module: the pink and red modules were positively correlated with FAH and SAH, respectively, and the blue, brown, and turquoise modules with FFH, SFH, and TFH, respectively. Hub genes of the pink/red modules were mainly NAC and MYB regulators of secondary wall and lignin synthesis, whereas those of the blue module were enriched for flowering related transcription factors, including the floral meristem identity gene *UrAP1* (g15350), which was specifically and highly expressed at FFH and almost silent in stem hooks, making it a promising candidate gene associated with peduncle reproductive identity. Studies in model plants have shown that *FD*, a bZIP transcription factor, binds the *AP1* promoter and transduces the flowering signal of the florigen *FT* (Yu et al. 2026). In our data, *UrFD*, which also belonged to the blue module, was significantly up-regulated at FFH and showed an expression pattern highly coordinated with *UrAP1*, suggesting that an *UrFD-UrAP1* regulatory module may be conserved in *U. rhynchophylla*. Integrating differential expression features, module-hub properties, gene co-expression trends, and Arabidopsis pathway conservation, we finally selected *UrAP1* as the main research target, and selected its upstream candidate regulator *UrFD* for subcellular localization, promoter cloning, and Y1H assays to verify the protein-DNA interaction between them.

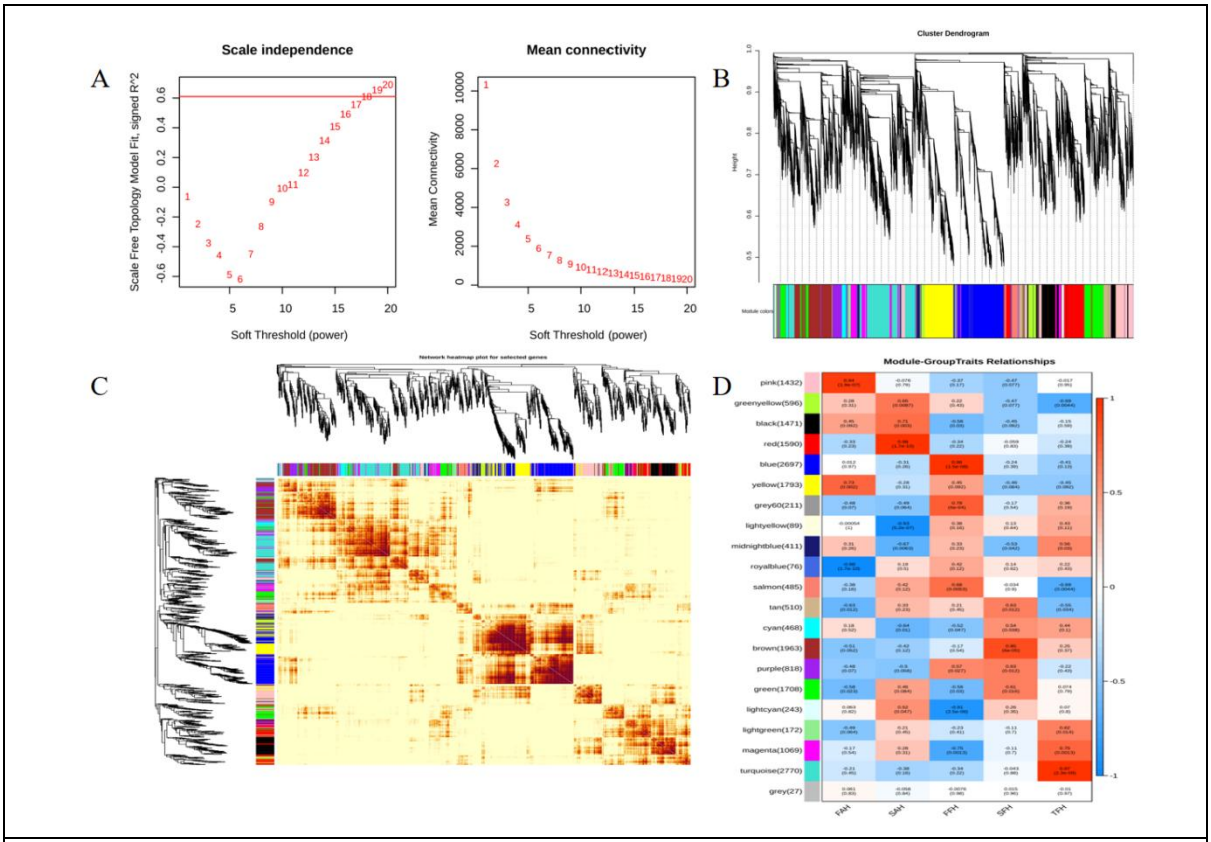


Fig. 10: Weighted gene co-expression network analysis (WGCNA). A: Determination of the soft-thresholding power (β). B: Hierarchical clustering dendrogram of genes. C: Network heatmap plot showing the topological overlap among selected genes. D: Module-trait relationships

3.10 Subcellular localization and yeast one-hybrid analysis

3.10.1 Subcellular localization of *UrAP1*

Transcription factors must be targeted to the nucleus to exert their functions. To verify the subcellular localization of *UrAP1*, an *UrAP1*-GFP fusion expression vector was constructed and used for Agrobacterium-mediated transient transformation of N. benthamiana leaves. Laser confocal scanning microscopy (Fig. 11) showed that the green fluorescence of the *UrAP1*-GFP fusion protein was specifically concentrated in the nucleus, whereas the empty GFP control was distributed in both the nucleus and the cytoplasm. This demonstrates that *UrAP1* is localized to the nucleus, consistent with the subcellular characteristics of a transcription factor and providing the cellular basis for its function as a transcriptional regulator.

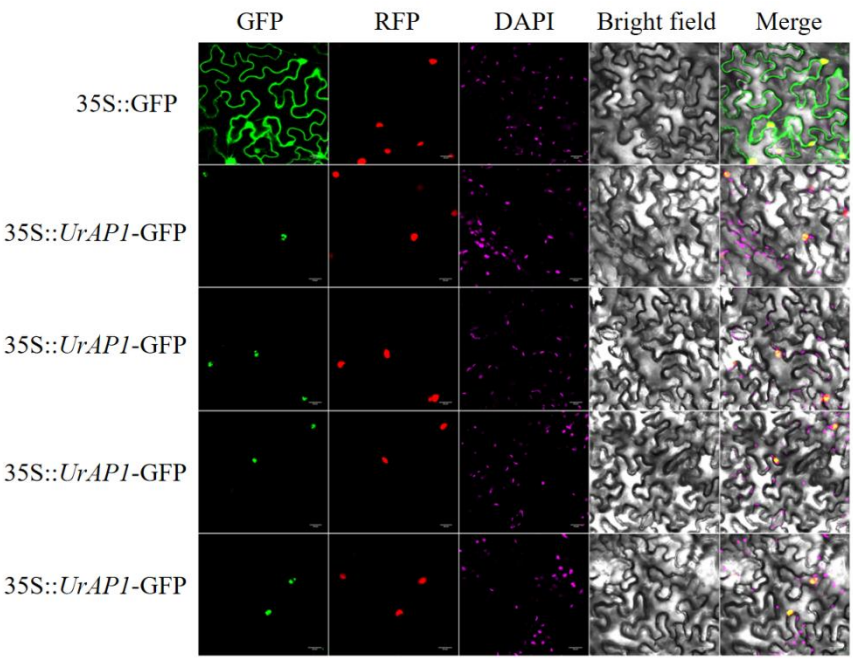


Fig. 11: Subcellular localization of *UrAP1*. The *UrAP1*-GFP fusion protein was transiently expressed in Nicotiana benthamiana leaf epidermal cells. GFP fluorescence (green), a nuclear marker (RFP, red), DAPI staining (blue/purple) and the bright-field image (BF) were captured, and the merged image is shown at the right. Bars = 20 μm.

3.10.2 Vector construction and yeast one-hybrid assay

The *UrAP1* promoter bait vector (pAbAi-*UrAP1*) and the *UrFD* prey plasmid (pGADT7-*UrFD*) were successfully constructed. In the bait self-activation test, a 500 ng/ml Aureobasidin A (AbA) concentration completely suppressed the self-activation of pAbAi-*UrAP1* and was therefore used as the working concentration (Fig. 12). On selective plates, the positive control grew normally, the negative control showed no colonies, and the co-transformed pAbAi-*UrAP1* + pGADT7-*UrFD* strain formed colonies at every dilution (Fig. 13), demonstrating that the *UrFD* protein directly binds the *UrAP1* promoter in vitro.

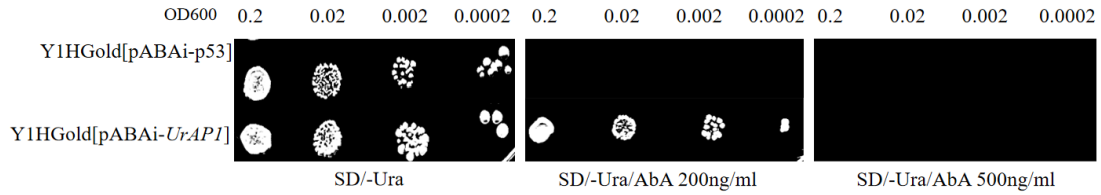


Fig. 12: Self-activation assay of the bait yeast strain.

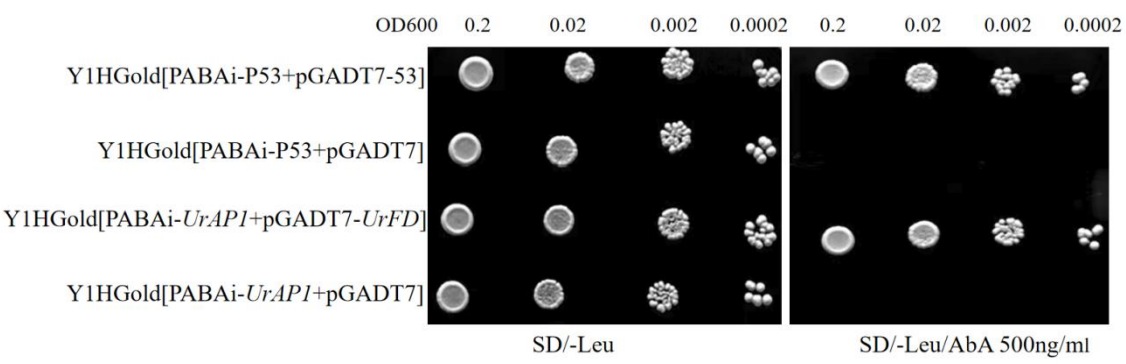


Fig. 13: Yeast one-hybrid assay verifying the binding of the *UrFD* protein to the *UrAP1* promoter.

4 Discussion

4.1 Fate separation of the two homologous axillary organs of *U. rhynchophylla* is supported by distinct transcriptomic backgrounds

Both the stem hook and the peduncle originate from axillary meristems, yet they differentiate into organs with completely different functions. The stem hook is a highly lignified climbing medicinal organ, whereas the peduncle is a reproductive support tissue. Our sample correlation analysis and PCA analysis indicated that the hook and peduncle samples formed two distinct clusters, and the organ identity was the main factor driving the global transcriptional differentiation. This is consistent with findings from other woody medicinal plants with modified stems, in which homologous-organ fate transitions are accompanied by large scale transcriptional reprogramming (Yang et al. 2019; Xiao et al. 2023).

During hook maturation, cell wall biosynthesis and phenylpropanoid biosynthesis were significantly enriched, in close agreement with anatomical studies showing that the hook develops from a lateral branch of the stem and progressively forms stem like lignified vascular tissues (Deng et al. 2021). In the WGCNA analysis, the red module, which was highly associated with the mature hook SAH, was enriched for a large number of NAC and MYB family hub genes. In woody plants, the NAC, MYB transcriptional molecular modules regulate secondary wall and xylem development (Fan et al. 2026); our results suggest that this pathway may play a central role in hook lignification in *U. rhynchophylla*.

Hormone signals are important endogenous factors regulating hook morphogenesis. Transcriptome results showed that during hook maturation, auxin response genes *SAUR* and *ARF* were upregulated, whereas ABA signaling gene *ABF* was downregulated. This expression pattern is consistent with endogenous hormone measurements during hook development, auxin content increases gradually while ABA content continuously decreases (Wan et al. 2025). Auxin is known to drive asymmetric cell expansion through cell-wall-loosening proteins, including expansins and xyloglucan endotransglycosylase/hydrolases (XTHs) (Zeng et al. 2024), and an auxin gradient across a bending organ can induce differential growth that forms hook like curvature (Wang et al. 2026). Auxin response factors can also fine tune the expression of lignin biosynthetic genes (Wang et al. 2024), therefore, the elevated auxin signaling during hook maturation may both generate the asymmetric growth underlying the hooked morphology and activate the lignification program. In agreement with this, KEGG enrichment showed that the phenylpropanoid pathway, which provides the monolignol precursors required for lignin biosynthesis was significantly enriched in mature hooks, indicating that phenylpropanoid metabolism contributes to the lignification of the stem hook during maturation.

4.2 Time-course reprogramming of sugar metabolism and hormone signals is associated with the reproductive transition of the peduncle

The peduncle and stem hook are homologous organs, but their developmental fate shifts toward reproductive growth, accompanied by large scale transcriptional reprogramming during flower bud initiation and flowering. STEM time-course clustering divided all peduncle DEGs into eight expression profiles, four of which were statistically significant. Genes in Profiles 0 and 1 were highly expressed at FFH and then continuously downregulated, and were significantly enriched for cell cycle, DNA replication, cytoskeleton assembly, starch sucrose metabolism, and hormone signal transduction, reflecting vigorous cell division in the flower-bud peduncle and a large requirement for carbohydrates to support the initial construction of reproductive tissues. Genes in Profiles 6 and 7 were progressively upregulated during semi-flowering and full flowering, and were enriched in pathways related to secondary metabolite synthesis and hormone modification, marking the developmental switch of the peduncle from cell proliferation to organ maturation. This time-course pattern is highly similar to transcriptomic features of floral-organ development in woody fruit trees such as longan and litchi (Huang et al. 2022; Wei et al. 2017), reflecting a certain conserved logic in the development of reproductive support structures in woody plants.

Sugars serve not only as energy and carbon skeleton sources but also as signaling molecules regulating the floral transition. Trehalose-6-phosphate (T6P) is a core signaling molecule linking sucrose metabolism to flowering signals, and *TPS* is the key enzyme for T6P synthesis; the *Arabidopsis tps1* mutant displays a late-flowering phenotype (Fichtner et al. 2025). In this study, KEGG results showed that the starch sucrose metabolism pathway was significantly enriched in Profile 0, and that *TPS* and the starch synthesis gene *glgC* were significantly upregulated in the flower-bud peduncle, suggesting that T6P mediated sugar signaling participates in the establishment of peduncle reproductive identity. By contrast, in the tender stem hooks, hexose metabolism genes such as hexokinase *HK* were highly expressed, prioritizing hexose metabolism to provide carbon sources for rapid elongation and lignification of the climbing organ, reflecting fundamentally different

carbon-metabolism reprogramming patterns in these two homologous organs (Vanderwall al. 2023).

Multiple phytohormone signaling pathways undergo time-course switching at different peduncle stages. The KEGG plant hormone signal transduction pathway was significantly enriched in Profiles 0 and 1. The GA pathway genes *GID2* and *DELLA* were significantly upregulated at FFH, whereas the JA and ethylene pathway genes *MYC2* and *ERF1* were mainly upregulated during SFH-TFH. Endogenous hormone measurements likewise confirmed that GA content continuously increases during peduncle development and peaks at full flowering, promoting floral-organ differentiation and opening (Wan al. 2025). Together, these results indicate that peduncle reproductive development is not regulated by a single hormone, but rather by coordinated time-course switching of the sugar metabolism network and multiple hormone signaling pathways, jointly accomplishing the fate transition of the peduncle from an ordinary stem like support structure to a reproductive organ.

4.3 The conserved *UrFD-UrAP1* regulatory module is likely involved in peduncle reproductive development

The *FT-FD-AP1* cascade is the classical flowering pathway in model plants, the florigen *FT* is transported to the shoot apex, forms a protein complex with the bZIP transcription factor *FD*, and *FD* directly binds the *AP1* promoter to activate its transcription. *AP1*, as a floral meristem identity gene, further initiates downstream floral organ differentiation programs (Gao al. 2025; Tian et al. 2026). This pathway is functionally conserved in perennial woody plants such as poplar and longan, but also shows species specific divergence (Jue et al. 2019). Our WGCNA results showed that the blue module was strongly positively correlated with FFH; within this module, the hub gene *UrAP1* was specifically and highly expressed in the flower-bud peduncle and was almost silent in stem hooks. The upstream candidate gene *UrFD* also belonged to the blue module, and the two showed highly coordinated expression patterns. Subcellular localization confirmed that *UrAP1* was targeted to the nucleus, consistent with the subcellular characteristics of MADS-box transcription factors and providing the cellular basis for transcriptional regulation (Xu et al. 2025). In vitro Y1H assays demonstrated that the *UrFD* protein could directly bind the *UrAP1* promoter, suggesting that a conserved *UrFD* mediated transcriptional activation unit on *UrAP1* exists in *U. rhynchophylla*. This module may serve as a key regulatory component associated with the initiation of reproductive development in the peduncle.

The floral repressor *UrSVP* was highly expressed in stem hooks. SVP-type MADS-box proteins can repress flowering genes such as *FT, SOC1*, and *AP1* in vegetative tissues, preventing the transition from vegetative to floral meristems (Chen et al. 2026). We therefore propose that the high expression of *UrSVP* in stem hooks represses the activation of the flowering program, prevents hooks from differentiating toward the peduncle fate, and maintains the identity of the stem hook as a vegetative climbing organ (Zhang et al. 2023). This hypothesis provides a reasonable molecular level model for explaining how a homologous axillary meristem differentiates into two entirely different organs (Zhu et al. 2020).

4.4 Limitations and future perspectives

This study provides a multi-stage transcriptomic view of the divergence between stem hooks and peduncles in *U. rhynchophylla*, but several limitations should be acknowledged. First, the transcriptome analysis is descriptive, and the evidence for the *UrFD-UrAP1* module is currently limited to in vitro assays. Second, Y1H demonstrates DNA binding only; whether *UrFD* transactivates the *UrAP1* promoter requires transient transactivation assays and electrophoretic mobility shift assays to define the binding site. Third, although the classical flowering model involves the *FT-FD* complex, the interaction between *UrFT* and *UrFD* has not been tested, and the presumed function of the module in the peduncle versus the shoot apical meristem remains to be established. Fourth, no transgenic or phenotypic evidence is yet available. Fifth, all plant materials were collected from a single cultivated nursery base; gene expression profiles may be influenced by local environmental conditions, and multi-site sampling is needed in future work to validate the robustness of our observations. Future work should functionally dissect the *UrFD-UrAP1* and *UrSVP* modules by stable transformation.

5 Conclusion

In summary, this study generated a multi-stage comparative transcriptome of the two homologous axillary organs of *U. rhynchophylla*, the medicinal stem hook and the reproductive peduncle, across five developmental stages, and showed that their divergent fates are underpinned by distinct, stage specific transcriptional programs. The transcriptomes of stem hooks and peduncles were clearly separated, with organ identity, rather than within organ developmental timing, representing the dominant source of divergence. Hook maturation was characterized by activation of cell wall construction and phenylpropanoid biosynthesis, auxin signal activation,

ABA signal attenuation, and NAC, MYB driven secondary wall lignification. In the peduncle, the reproductive transition involved time-course reprogramming of sugar metabolism and multiple hormone signaling pathways, together with significant upregulation of the flowering integrators *UrFT, UrSOC1, UrFD* and *UrAP1* at the flower-bud stage. WGCNA further identified a flower-bud-specific blue module with *UrAP1* as its core hub gene; subcellular localization and yeast one-hybrid assays provided in vitro evidence that *UrFD* binds the *UrAP1* promoter, supporting a conserved *UrFD-UrAP1* regulatory module that is likely involved in peduncle reproductive development. Conversely, the floral repressor *UrSVP* was highly expressed in stem hooks, suggesting that repression of the flowering program helps maintain the vegetative identity of the hook. Collectively, these findings provide a transcriptomic framework and candidate gene resources for understanding how homologous structures acquire distinct developmental fates, and a basis for the targeted regulation of the medicinal organ and molecular breeding of *U. rhynchophylla*.

Supplementary Information

Online Resource 1: Primers used in real-time fluorescence quantitative PCR.

Online Resource 2: Specific primers for the *UrAP1* promoter sequence.

Online Resource 3: Specific primers of *UrFD*.

Online Resource 4: Quality assessment of transcriptome sequencing data.

Online Resource 5: Supplementary figures S1-S4, showing the GO and KEGG diagrams of clusters 0, 1, 6, and 7.

Acknowledgements We appreciate Yuguo Wei from Feiteng Chinese Herbal Medicine Planting Professional Cooperative in Rong'an County, Liuzhou, Guangxi, for providing plant materials and support for this work.

Author contributions JS conceived and designed the research and wrote the original draft of the manuscript. JS, YQ, YL, CY conducted the experiments. WL, LL, QT, LG, HY, and YH participated in data analysis and assisted in reviewing and editing the manuscript. GT, SW, FQ and LW reviewed and revised the manuscript. All authors discussed the results, contributed to the revision of the manuscript, and approved the final version for submission.

Funding This work was supported by the Guangxi Natural Science Foundation Project (2025GXNSFBA069172, 2026GXNSFAA00640239), the National Natural Science Foundation Project (82360753, 82660872, 81903752), and the self-funded project of Guangxi Traditional Chinese Medicine Administration Bureau (CXZYA20250005).

Data availability The raw sequencing data from this study have been deposited in the Genome Sequence Archive in BIG Data Center (https://bigd.big.ac.cn/),Beijing Institute of Genomics (BIG), Chinese Academy of Sciences, and the formal accession number will be provided upon acceptance.

Declarations

Ethics approval and consent to participate The plant materials of *Uncaria rhynchophylla* used in this study were collected from the cultivated nursery base in Sanchadun, Mabucun, Banlan Town, Rong'an County, Liuzhou City, Guangxi, China. Sampling was permitted by the management of the nursery base. All sampling procedures complied with relevant national legislation of China. No wild protected plant resources were involved in this study.

Conflict of interest The authors declare that they have no known competing financial interests or personal relationships that could influence the work reported in this study.

References:

Abe M, Kobayashi Y, Yamamoto S, Daimon Y, Yamaguchi A, Ikeda Y, Ichinoki H, Notaguchi M, Goto K, Araki T (2005) FD, a bZIP protein mediating signals from the floral pathway integrator FT at the shoot apex. Science (New York, N.Y.), 309(5737), 1052-1056. https://doi.org/10.1126/science.1115983

Anders S, Huber W (2010) Differential expression analysis for sequence count data. Genome biology, 11(10), R106. https://doi.org/10.1186/gb-2010-11-10-r106

Ashburner M, Ball C A, Blake J A, Botstein D, Butler H, Cherry J M, Davis A P, Dolinski K, Dwight S S, Eppig J T, Harris M A, Hill D P, Issel-Tarver L, Kasarskis A, Lewis S, Matese J C, Richardson J E, Ringwald M, Rubin G M, Sherlock G (2000) Gene ontology: tool for the unification of biology. The Gene Ontology Consortium. Nature genetics, 25(1), 25-29. https://doi.org/10.1038/75556

Cao R, Wang Y, Zhou Y, Zhu J, Zhang K, Liu W, Feng F, Qu W (2024) Advanced researches of traditional uses,

phytochemistry, pharmacology, and toxicology of medical Uncariae Ramulus Cum Uncis. Journal of ethnopharmacology, 325, 117848. https://doi.org/10.1016/j.jep.2024.117848

Chen L, Chen J, Zhong H, Yang Z, Fang C, Kong F, Liu B, Lu S (2026) Rewiring the SVP-AGL24 module into a flowering-promoting cascade via legume-specific E1 repressors in soybean. Journal of integrative plant biology, 10.1111/jipb.70404. Advance online publication. https://doi.org/10.1111/jipb.70404

Cock P J, Fields C J, Goto N, Heuer M L, Rice P M (2010) The Sanger FASTQ file format for sequences with quality scores, and the Solexa/Illumina FASTQ variants. Nucleic acids research, 38(6), 1767-1771. https://doi.org/10.1093/nar/gkp1137

Dai Y, Yuan L, Zhang S, Wang J, Xie S, Zhao M, Chen G, Sun R, Wang C (2019) Comprehensive Evaluation for Cold Tolerance in Wucai (Brassica campestris L.) by the Performance Index on an Absorption Basis (PIabs). Agronomy, 9(2), 61. https://doi.org/10.3390/agronomy9020061

Deng K P, Yang S W, Yang X W, Zhang Y K (2021) Anatomical study on the morphological development of the hook organ in *Uncaria rhynchophylla*. Guihaia. 41(12):1981-1987.

Díaz-Riquelme J, Martínez-Zapater J M, Carmona M J (2014) Transcriptional analysis of tendril and inflorescence development in grapevine (Vitis vinifera L.). PloS one, 9(3), e92339. https://doi.org/10.1371/journal.pone.0092339

Dobin A, Davis C A, Schlesinger F, Drenkow J, Zaleski C, Jha S, Batut P, Chaisson M, Gingeras T R (2013) STAR: ultrafast universal RNA-seq aligner. Bioinformatics (Oxford, England), 29(1), 15-21. https://doi.org/10.1093/bioinformatics/bts635

Emonet A, Pérez-Antón M, Neumann U, Dunemann S, Huettel B, Koller R, Hay A (2024) Amphicarpic development in Cardamine chenopodiifolia. The New phytologist, 244(3), 1041-1056. https://doi.org/10.1111/nph.19965

Ernst J, Bar-Joseph Z (2006) STEM: a tool for the analysis of short time series gene expression data. BMC bioinformatics, 7, 191. https://doi.org/10.1186/1471-2105-7-191

Fan G, Jiang J, Cheng Z, Ma F, Sun Z, Li Z, Qi Y, Qu G, Jiang T (2026) A MYB-Related Transcriptional Module Cooperatively Represses Xylem Development in Poplar. Plant biotechnology journal, 10.1111/pbi.70745. Advance online publication. https://doi.org/10.1111/pbi.70745

Fichtner F (2025) Trehalose 6-phosphate-a central regulator at the crossroads of sugar signalling, metabolism, and development. The New phytologist, 248(5), 2243-2250. https://doi.org/10.1111/nph.70533

Gao H, Ding N, Wu Y, Yu D, Zhou S Z, Stolze S C, Vincent C, Rodríguez Maroto G, de Los Reyes P, Harzen A, Cerise M, da Silveira Falavigna V, Li E, Timmers T, Neumann U, Nakagami H, Hu J Y, Chai J, Coupland G (2025) Florigen activation complex forms via multifaceted assembly in Arabidopsis. Nature, 648(8094), 686-695. https://doi.org/10.1038/s41586-025-09704-6

Guo Q, Si X, Shi Y, Yang H, Liu X, Liang H, Tu P, Zhang Q (2019) Glucoconjugated Monoterpene Indole Alkaloids from *Uncaria rhynchophylla*. Journal of natural products, 82(12), 3288-3301. https://doi.org/10.1021/acs.jnatprod.9b00490

Hartley S W, Mullikin J C (2015) QoRTs: a comprehensive toolset for quality control and data processing of RNA-Seq experiments. BMC bioinformatics, 16(1), 224. https://doi.org/10.1186/s12859-015-0670-5

Huang S, Qiao Y, Lv X, Li J, Han D, Guo D (2022) Transcriptome sequencing and DEG analysis in different developmental stages of floral buds induced by potassium chlorate in Dimocarpus longan. Plant biotechnology (Tokyo, Japan), 39(3), 259–272. https://doi.org/10.5511/plantbiotechnology.22.0526a

Jue D, Sang X, Liu L, Shu B, Wang Y, Liu C, Wang Y, Xie J, Shi S (2019) Comprehensive analysis of the longan transcriptome reveals distinct regulatory programs during the floral transition. BMC genomics, 20(1), 126. https://doi.org/10.1186/s12864-019-5461-3

Kanehisa M, Araki M, Goto S, Hattori M, Hirakawa M, Itoh M, Katayama T, Kawashima S, Okuda S, Tokimatsu T, Yamanishi Y (2008) KEGG for linking genomes to life and the environment. Nucleic acids research, 36(Database issue), D480-D484. https://doi.org/10.1093/nar/gkm882

Kuang Y, Zhu M, Gu H, Tao Y, Huang H, Chen L (2024) Alkaloids in Uncaria rhynchophylla improves AD pathology by restraining CD4+ T cell-mediated neuroinflammation via inhibition of glycolysis in APP/PS1 mice. Journal of ethnopharmacology, 331, 118273. https://doi.org/10.1016/j.jep.2024.118273

Liang J H, Wang C, Huo X K, Tian X G, Zhao W Y, Wang X, Sun C P, Ma X C (2020) The genus Uncaria: A review on phytochemical metabolites and biological aspects. Fitoterapia, 147, 104772. https://doi.org/10.1016/j.fitote.2020.104772

Liu X, Chen W, Li L, Mu D, Wilson I W, Huang X, Xiang Y, Zhu L, Pan L, Qiu D, Tang Q (2025). Identification and Functional Characterization of a Geraniol Synthase UrGES from Uncaria rhynchophylla. Plants (Basel,

Switzerland), 14(15), 2273. https://doi.org/10.3390/plants14152273
Mu D, Wan L, Shao Y, Pan L, Liu X, Wilson I W, Qing Z, Zhou Y, Lu Y, He Y, Zhu L, Fu J, Wei S, Ma X, Song C, Qiu D, Tang Q (2026) The genome of the medicinal plant Uncaria rhynchophylla provides new insights into monoterpenoid indole alkaloid metabolism and its molecular regulatory mechanism. Molecular horticulture, 6(1), 9. https://doi.org/10.1186/s43897-025-00187-7
National Pharmacopoeia Committee (2025) Chinese Pharmacopoeia. China Pharmaceutical Science and Technology Press, Beijing, 277
Niu Y, Chen L, Su C, Wang L (2026) Florigen FT: A Signaling Hub Connecting Environmental Cues and Developmental Regulation. Chinese Bulletin of Botany, 61(1): 1-8.https://doi.org/10.11983/CBB25203
Pertea M, Pertea G M, Antonescu C M, Chang T C, Mendell J T, Salzberg S L (2015) StringTie enables improved reconstruction of a transcriptome from RNA-seq reads. Nature biotechnology, 33(3), 290-295. https://doi.org/10.1038/nbt.3122T
Qin J X, Hong Y, Zhao L Y, Wang C Q, Fang X, Liang S (2024) The basic chemical substances of total alkaloids of *Uncaria rhynchophylla* and their anti-neuroinflammatory activities. Journal of Asian natural products research, 26(6), 765-771. https://doi.org/10.1080/10286020.2024.2315211
Ren J, Duan Y, Li R, Zhang X, Shi Y, Zhou S, Xie K, Wu X, Irish V F, Deng X, Zhang F, Guo W (2025) Transcriptional regulation of thorn tip sclerification in plants. Proceedings of the National Academy of Sciences of the United States of America, 122(39), e2510775122. https://doi.org/10.1073/pnas.2510775122
Reuter J, Spacek D, Snyder M (2015) High-throughput sequencing technologies. Mol Cell, 58(4):586-597. https://doi.org/10.1016/j.molcel.2015.05.004
Shao Y, Mu D, Zhou Y, Liu X, Huang X, Wilson I W, Qi Y, Lu Y, Zhu L, Zhang Y, Qiu D, Tang Q (2024) Genome-Wide Mining of CULLIN E3 Ubiquitin Ligase Genes from Uncaria rhynchophylla. Plants (Basel, Switzerland), 13(4), 532. https://doi.org/10.3390/plants13040532
Singh V K, Mangalam A K, Dwivedi S, Naik S (1998) Primer premier: program for design of degenerate primers from a protein sequence. BioTechniques, 24(2), 318-319. https://doi.org/10.2144/98242pf02
Tian S, Luo X, Cui B, He Y (2026) Auto-Downregulation of the Florigen FT Production Prevents Precocious Flowering in Plants. Advanced science (Weinheim, Baden-Wurttemberg, Germany), 13(55), e22307. https://doi.org/10.1002/advs.202522307
Vanderwall M, Gendron J M (2023). HEXOKINASE1 and glucose-6-phosphate fuel plant growth and d evelopment. Development (Cambridge, England), 150(20), dev202346. https://doi.org/10.1242/dev.202 346
Wan L, Ji X, Pan L, Song L, Liang W, Yang C, Yan Z, Zhang Z, Wei S (2025) Variations in content of endogenous phytohormones in the hook and peduncle of *Uncaria rhynchophylla* at different developmental stages. Guangxi Sciences 32:255-265
Wang W, Li Y, Cai C, Zhu Q (2024) Auxin response factors fine-tune lignin biosynthesis in response to mechanical bending in bamboo. The New phytologist, 241(3), 1161-1176. https://doi.org/10.1111/nph.19398
Wang X, Cai X, Huo H, Chen H (2026) Gravity sensing in plants. The New phytologist, 251(3), 996-1012. https://doi.org/10.1111/nph.71324
Wei Y, Dong C, Zhang H, Zheng X, Shu B, Shi S, Li W (2017) Transcriptional changes in litchi (Litchi chinensis Sonn.) inflorescences treated with uniconazole. PloS one, 12(4), e0176053. https://doi.org/10.1371/journal.pone.0176053
Wu Q, Wu Y, Li R, Cao H, Li Z, Li Q, Zhou L (2025) Research Progress on the Regulation of Plant Floral Organ Development by the MADS-box Gene Family. International journal of molecular sciences, 26(18), 8946. https://doi.org/10.3390/ijms26188946
Xiao F, Zhao Y, Wang X, Sun Y (2023) Comparative Transcriptome Analysis of Gleditsia sinensis Thorns at Different Stages of Development. Plants (Basel, Switzerland), 12(7), 1456. https://doi.org/10.3390/plants12071456
Xu S, H E, Cai Y, Xie Z, Luo X, Zhan L, Tang W, Wang Q, Liu B, Wang R, Xie W, Wu T, Xie L, Yu G (2024) Using clusterProfiler to characterize multiomics data. Nature protocols, 19(11), 3292-3320. https://doi.org/10.1038/s41596-024-01020-z
Xu X, Neumann M, Carew F, Chen P, Braeuning C, Zubieta C, Muino J M, Smaczniak C, Kaufmann K (2025) AP1 is a pioneer transcription factor that programmes cell fate through MADS-domain protein tetramerisation. Genome biology, 26(1), 418. https://doi.org/10.1186/s13059-025-03884-0
Yang Q, Liu S, Han X, Ma J, Deng W, Wang X, Guo H, Xia X (2019) Integrated transcriptome and miRNA

631 analysis uncovers molecular regulators of aerial stem-to-rhizome transition in the medical herb
632 *Gynostemma pentaphyllum*. BMC genomics, 20(1), 865. https://doi.org/10.1186/s12864-019-6250-8
633 Yang W, Ip S P, Liu L, Xian Y F, Lin Z X (2020) *Uncaria rhynchophylla* and its Major Constituents on Central
634 Nervous System: A Review on Their Pharmacological Actions. Current vascular pharmacology, 18(4),
635 346-357. https://doi.org/10.2174/1570161117666190704092841
636 Zeng H Y, Deng S, Jin C, Shang Z, Chang L, Wang J, Han X, Wang A, Jin D, Wang Y, He H, Li L, Deng X W,
637 Wei N (2024) Origin and evolution of auxin-mediated acid growth. Proceedings of the National Academy
638 of Sciences of the United States of America, 121(51), e2412493121.
639 https://doi.org/10.1073/pnas.2412493121
640 Zhang D, Zhou H, Zhang Y, Zhao Y, Zhang Y, Feng X, Lin H (2025) Diverse roles of MYB transcription factors
641 in plants. Journal of integrative plant biology, 67(3), 539-562. https://doi.org/10.1111/jipb.13869
642 Zhang Z, Hu Q, Gao Z, Zhu Y, Yin M, Shang E, Liu G, Liu W, Hu R, Cheng H, Chong X, Guan Z, Fang W,
643 Chen S, Sun B, He Y, Chen F, Jiang J (2023) Flowering repressor *CmSVP* recruits the TOPLESS
644 corepressor to control flowering in chrysanthemum. Plant physiology, 193(4), 2413-2429.
645 https://doi.org/10.1093/plphys/kiad476
646 Zhao Q, Zhang M, Gu L, Yang Z, Li Y, Luo J, Zhang Y (2024) Transcriptome and volatile compounds analyses
647 of floral development provide insight into floral scent formation in *Paeonia lactiflora* 'Wu Hua Long Yu'.
648 Frontiers in plant science, 15, 1303156. https://doi.org/10.3389/fpls.2024.1303156
649 Zhong R, Lee C, Haghighat M, Ye Z H (2021) Xylem vessel-specific SND5 and its homologs regulate
650 secondary wall biosynthesis through activating secondary wall NAC binding elements. The New
651 phytologist, 231(4), 1496-1509. https://doi.org/10.1111/nph.17425
652 Zhu Y, Wagner D (2020) Plant Inflorescence Architecture: The Formation, Activity, and Fate of Axillary
653 Meristems. Cold Spring Harbor perspectives in biology, 12(1), a034652.
654 https://doi.org/10.1101/cshperspect.a034652

Supplementary Files

This is a list of supplementary files associated with this preprint. Click to download.

- SupplementaryInformation.zip